Robot Path Planning for Monitoring Dynamic Environment by Predictive Uncertainty Minimization Using Gaussian Process Regression

Tian Gao*, Nattaon Techasarntikul†, Yuichi Ohsita†, Hideyuki Shimonishi†
*Graduate School of Information Science and Technology, Osaka University, Japan
u151056j@ecs.osaka-u.ac.jp
†D3 Center, Osaka University, Japan
techa.nattaon.cmc@osaka-u.ac.jp, yuichi.ohsita.cmc@osaka-u.ac.jp, shimonishi.cmc@osaka-u.ac.jp

***Abstract*—In environmental monitoring, traditional methods primarily focus on collecting as much spatial information as possible to construct a more accurate static model of the environment. However, these methods fail to account for the fact that environmental factors, such as temperature, can vary over time during monitoring, making it difficult for robots efficiently capture temporal dynamics of each region across the entire spatial area. This paper addresses these challenges by applying a spatio-temporal Gaussian Process Regression (GPR) model, which estimates not only the environmental conditions of unobserved regions but also their associated uncertainties based on observed data, considering time variations. Building upon this model, we propose a method called Predictive Uncertainty Minimization (PUM), which controls the robot's trajectory to minimize future uncertainties. Through simulation using the data set obtained in the real-world environment, we show that PUM consistently maintains lower uncertainty levels, reducing overall uncertainty by 7.91% and 9.25% compared to the method following a pre-defined path and the method continuously moving to the point with the highest uncertainty, respectively.**

***Index Terms*—environmental monitoring, Gaussian Process Regression, uncertainty, model predictive control, spatiotemporal kernel, informative path planning**

I. Introduction

Efficient environmental monitoring in dynamic environments is a critical task in a variety of fields, including disaster response [1], smart building management [2], and precision agriculture [3]. By monitoring the dynamic environment, we can make decisions suitable to current situation; for example, people can be guided to a more comfortable place by tracking the current temperature at each location [4]. Environmental monitoring typically requires continuous and accurate data collection in wide areas to make informed decisions. However, deploying additional sensors is impractical or cost-prohibitive to cover wide areas.

To address this challenge, robots have emerged as an effective solution for such tasks due to their ability to move autonomously and collect real-time data from diverse environments. The mobility of robots enables them to access areas that may be difficult or dangerous for humans, making them valuable tools in dynamic and unpredictable environments [5].

An important aspect of mobile robots for environmental monitoring is path planing. Traditional path planning methods typically prioritize efficiency, such as minimizing travel distance or energy consumption, without considering the value of the data collected along the way. In contrast, Informative Path Planning (IPP) shifts focus to maximizing the acquisition of environmental data and evaluates potential paths based on the expected information gain from unexplored areas [6]. A key component of IPP is the use of Gaussian Process Regression (GPR), which models environmental features and provides probabilistic predictions along with their uncertainties. By using the uncertainties, a path passing the regions with higher uncertainties is obtained. As the robot collects the data from these regions, the model of the environmental features become more accurate. Hitz et al. proposed a method to calculate the informative path in continuous space by optimizing a parameterized path [7]. Fentanes et al. also discussed path planning for 3D soil modeling and demonstrated that utilizing uncertainty as a reward function for robot exploration leads to more efficient data collection [8]. Geng et al. proposed active information gathering of a 3D surface based on IPP [9].

Most of the existing work on IPP focused on collecting information required for modeling the environment. Therefore, they maximize information gain within limited resources such as time, path length, or energy and do not consider the dynamic environment where features change over time. In contrast, this paper addresses applications that need real-time information on the current situation at each location. To collect current information, robots are used to perform long-term monitoring. The environmental features may change during the robot's movement, which means the past observations may be no longer useful, and new observations may be required to follow the real-time changes. Therefore, we need a method to control robots to collect the information required to follow real-time changes, considering dynamic environments whose features change over time.

In this paper, we propose a path planning method called Predictive Uncertainty Minimization (PUM), which leverages a spatio-temporal GPR model designed to account for both spatial and temporal correlations between monitored features.

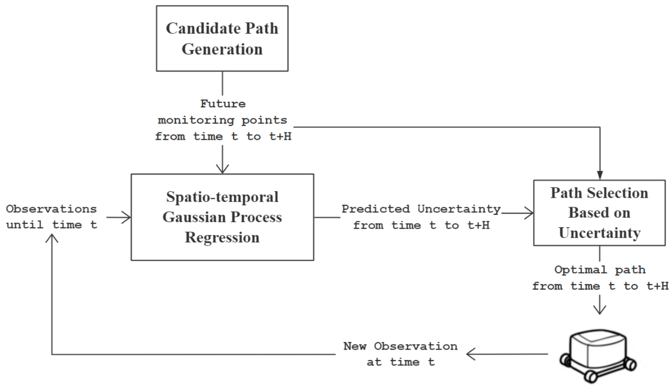

Fig. 1: Overview of predictive uncertainty minimization

The spatio-temporal GPR model tracks the increasing uncertainty in unobserved regions as time progresses. PUM generates the possible candidate monitoring paths, predicts the future uncertainty for each case by using the spatio-temporal GPR model, and selects the one whose uncertainty is the lowest. By continuing these steps, PUM allows the monitoring robots to continuously collect information to keep uncertainty low considering the dynamic environment.

Through experiments conducted with real-world temperature data, we show that PUM can effectivetly collect the information required to track environmental changes. In addition, we demonstrate that PUM outperforms the method of using the fixed path or continuously selecting the most uncertain points without considering future uncertainty.

II. Proposed Method

A. Overview

Figure 1 presents an overview of our method which utilizes the Spatio-Temporal Gaussian Process (ST-GPR). ST-GPR captures both spatial and temporal correlations within the data, allowing for predictions of the environmental features with their uncertainties.

In PUM, we first generate candidate paths from time t to $t+H$ at time t. By using the environmental data collected up to time t and the future monitoring points on each candidate path, ST-GPR is employed to predict the uncertainty of the environment from t to $t+H$. Based on these predicted uncertainties, we select the optimal path that minimizes the uncertainty from t to $t+H$. After obtaining the information at time t, we perform the same steps to obtain the path from $t+1$ to $t+1+H$. By continuing the above steps, we continuously move a robot to monitor the environment.

In the rest of this section, we explain the details of ST-GPR and PUM.

B. Spatio-Temporal GPR Model

In this paper, we address the challenge of monitoring dynamic environments by introducing a model capable of predicting environmental changes over both time and space. This model estimates the values at each location and time point, accounting for spatial and temporal correlations within the data. We denote $y(\mathbf{z},t)$ as the values at the location $\mathbf{z}$ and time t. $y(\mathbf{z},t)$ can be represented by

$$y(\mathbf{z},t) = \bar{\mathbf{y}} + \Delta y(\mathbf{z},t) \tag{1}$$

where

$$\bar{\mathbf{y}} = \frac{\sum_{\mathbf{z}\in Z, t\in T} y(\mathbf{z},t)}{|Z|\times|T|}. \tag{2}$$

where Z is the set of locations and T is the set of time slots we need to monitor. We can estimate $\bar{\mathbf{y}}$ by calculating the average of the monitored values. By focusing on $\Delta y(\mathbf{z},t)$, we model the values that depend on location and time.

To model $\Delta y(\mathbf{z},t)$, we use Gaussian Process Regression (GPR), a non-parametric Bayesian method widely adopted for path planning due to its ability to model and predict both mean values and uncertainty in environmental features. GPR is particularly effective in dynamic and partially observable conditions because it provides a probabilistic model that informs decision-making and allows the robot to focus on regions that maximize information gain.

We introduce a spatial-temporal GPR, that captures both spatial and temporal correlations. In this model, the mean μ and the variance σ^2 of $\Delta y(\mathbf{z},t)$ are modeled as a function of the new observation point $\mathbf{x}^* = (\mathbf{z},t)$.

$$\mu(\mathbf{x}^*) = k_{ST}(\mathbf{x}^*,\mathbf{X})K^{-1}\Delta y(\mathbf{z},t) \tag{3}$$

$$\sigma^2(\mathbf{x}^*) = k_{ST}(\mathbf{x}^*,\mathbf{x}^*) - k_{ST}(\mathbf{x}^*,\mathbf{X})K^{-1}k_{ST}(\mathbf{X},\mathbf{x}^*) \tag{4}$$

where $\mathbf{X}$ consists of previously observed locations and times, the vector $\mathbf{y}$ comprises the corresponding observed values. $k_{ST}(\mathbf{x}_i,\mathbf{x}_j)$ is the kernel function that defines the spatial and temporal relationships between the data. The matrix K is the covariance matrix derived from applying the kernel function to all pairs of points in $\mathbf{X}$. The mean value of predicted temperature $\hat{y}(\mathbf{x}^*)$ at the point $\mathbf{x}^*$ is then represented as $\bar{\mathbf{y}} + \mu(\mathbf{x}^*)$.

We define the kernel function $k_{ST}(\mathbf{x}_i,\mathbf{x}_j)$ which captures both spatial and temporal dependencies between two points $\mathbf{x}_i = (\mathbf{z}_i, t_i)$ and $\mathbf{x}_j = (\mathbf{z}_j, t_j)$ by

$$k_{ST}(\mathbf{x}_i,\mathbf{x}_j) = \sigma_0^2 \cdot \exp\left(-\frac{\|\mathbf{z}_i - \mathbf{z}_j\|^2}{2\cdot l_{\text{space}}^2}\right)\cdot \exp\left(-\frac{|t_i - t_j|}{l_{\text{time}}}\right) \tag{5}$$

where σ_0^2 acknowledges the presence of noise in the collection of real-world data, accounting for the noise in the observations, and l_{space} and l_{time} are parameters. This function accounts for spatial proximity and temporal continuity simultaneously; the spatial term indicates that points closer together are more strongly correlated, whereas the temporal term captures how the correlation decays over time.

An important aspect of ST-GPR is that it can predict the uncertainty $\sigma(\mathbf{x}^*)$ without requiring actual observations at future points. This means that we can predict uncertainty only by selecting the future monitoring points.

C. Predictive Uncertainty Minimization

In this section, we propose a path-planning method called Predictive Uncertainty Minimization (PUM). PUM is based on the principles of Model Predictive Control (MPC), where an optimization problem is solved over a finite horizon and only the first step of the solution is implemented. Once a new observation is obtained, the optimization problem is solved again. By continuing the above steps, the MPC achieves adaptive control based on predicted future states [10].

In PUM, we define an uncertainty function $U(\mathbf{X}, \mathcal{C})$ based on the uncertainties predicted from the ST-GPR model. This function evaluates the total uncertainty over a future path from the current time t to the horizon $t + H$, considering the combined effect of previously observed points ($\mathbf{X}$) and planned sampling points ($\mathcal{C}$):

$$U(\mathbf{X}, \mathcal{C}) = \int_{t}^{t+H} \sum_{\mathbf{z} \in \mathbf{Z}} \sigma \left(\{\mathbf{z}, t\} | \mathbf{X}, \hat{\mathbf{X}}_{\mathcal{C}} \right) dt, \tag{6}$$

where $\mathbf{X}$ represents the set of path points sampled by the robot up to time t, while $\hat{\mathbf{X}}_{\mathcal{C}}$ denotes the planned sampling points $\mathcal{C}$ from time t to $t + H$. This function measures the potential deviation between the predicted and actual environmental values, independent of direct observations.

To identify the most informative path, PUM minimizes the total accumulated uncertainty over the future path from t to $t + H$, as defined by:

$$\mathcal{C}^* = \underset{\mathcal{C} \in \{c^N\}}{\arg\min} U(\mathbf{X}, \mathcal{C}) \tag{7}$$

In this equation, $\mathcal{C}^*$ is the optimal set of future path points, where c is a potential point sampled by the robot, and N is the total number of points along that candidate path. The path $\mathcal{C}^*$ is the optimal path that minimizes the uncertainty U, given the current path $\mathbf{X}$.

After obtaining $\mathcal{C}^*$, PUM moves the robot to the next point on this optimal path. Then, PUM performs the above steps again. By repeating these steps, PUM continuously moves the robots, considering the uncertainty in the future.

PUM operates in two key phases: candidate path generation and path selection based on uncertainty.

Candidate path generation: Assuming that the robot operates with a fixed scanning interval ΔT and moves within a speed range of $[v_{min}, v_{max}]$, we generate candidate paths by repeating the selection of the next monitoring points. The next monitoring points are obtained by calculating the area that the robot can reach in time ΔT. We regard each coordinate within this region as the candidate next monitoring point. Then, we calculate the further points by calculating the reachable regions from each of the candidate's next regions. By repeating the process until the monitoring points within the time horizon H are obtained, we generate all possible candidate paths. As the time horizon H becomes larger, the number of candidate paths increases drastically, which causes a large calculation time. One approach to reducing the calculation time is to sample a small number of paths. However, this paper focuses on the utilization of predictive uncertainty and the efficient sampling method for PUM is one of our future research topics.

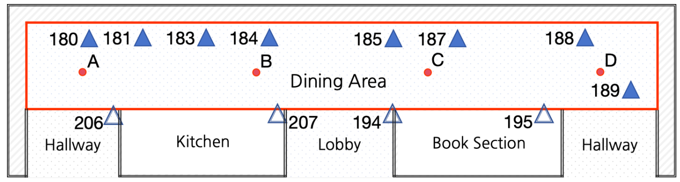

Fig. 2: Layout of 8 temperature sensors(dark-filled triangles) positioned in the dining area and 4 additional sensors(light-filled) in adjacent areas

Path selection based on uncertainty: After generation of candidate paths, PUM evaluates each of them by calculating $U(\mathbf{X}, \mathcal{C})$. The path with the smallest $U(\mathbf{X}, \mathcal{C})$ is then selected as the optimal path for the robot to follow.

III. Evaluation

A. Dataset

In this paper, we evaluate our method in the case of indoor temperature monitoring. For this evaluation, we utilize the data set collected by the temperature sensors installed at the Minoh Campus of Osaka University by Osaka University and Daikin Industries, Ltd. The dataset focuses on the dining area highlighted in red in Fig. 2, covering a dining space of 56 meters by 8 meters. Within this space, eight fixed temperature sensors were placed at a height of 2.2 meters from the floor to capture temperature data. Additionally, four more sensors were positioned in open areas outside the main dining space. The temperature values was measured at an interval of one minute, with a time lag between the sensors, meaning that they did not record all temperatures simultaneously.

In our experiment, we needed a reference dataset that captured the temperature variation across the entire monitored space, despite having limited sensor coverage. To achieve this, we utilized the GPR model that captures the spatial relation by using the following kernel function.

$$k_S(\mathbf{x}_i, \mathbf{x}_j) = \sigma_0^2 \cdot \exp\left(-\frac{\|\mathbf{z}_i - \mathbf{z}_j\|^2}{2 \cdot l_{\text{space}}^2} \right). \tag{8}$$

In this evaluation, we collected the most recent one-minute temperature measurements from the 12 sensors every 30 seconds and applied the GPR model with $\sigma_0 = 5$ and $l_{space} = 5$. Based on the interpolated values, we constructed the temperature dataset for the simulation environment with a grid size of 28x4 corresponding to the 56x8-meter area as shown in Fig. 3.

B. Parameter Settings

Two primary groups of parameters were considered in this experiment: the motion parameter of the robot and the parameters of the kernel function.

Based on the findings by Geng et al. [11], the optimal movement speed for a mobile robot performing temperature measurements was determined to be between 0.2 and 0.4

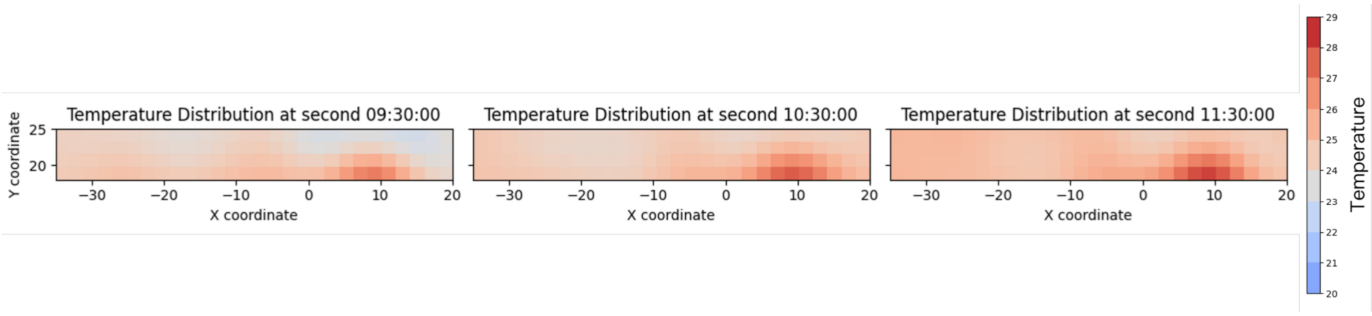

Fig. 3: Temperature distribution over time

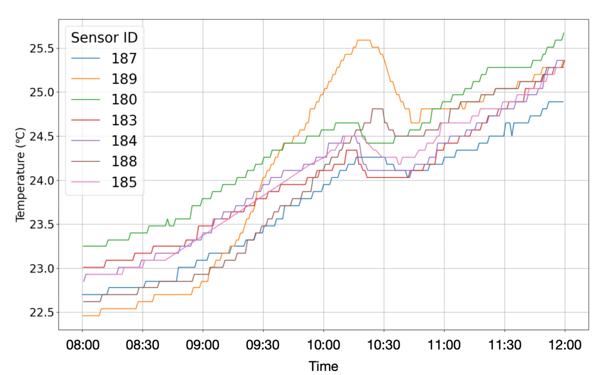

Fig. 4: Time variation of temperatures monitored by sensors

meters per second. In our evaluation, the robot's speed was constrained to between 0.1 (v_{min}) and 0.2 (v_{max}) grid units per second to correspond with the optimal movement speed in the real environment. Additionally, the robot was configured to measure the temperature every 20 seconds while in motion (ΔT). Furthermore, we set H in Eq. (6) to 40, meaning that the robot would predict the locations of the next two sampling points over the next 40 seconds.

Regarding Eq. (5), parameters such as l_{space}, l_{time}, and σ_0 are required to be adjusted within appropriate ranges to ensure that the model predictions closely matched the actual temperature variations. Varying the spatial gradient l_{space} controls how quickly the model's confidence decreases with distance, while the temporal gradient l_{time} dictates how fast the uncertainty rises over time. The parameter σ_0 affects the overall magnitude of uncertainty, influencing both the rate and the maximum value of uncertainty in the model. Together, these parameters play a crucial role in balancing the model's predictive power and uncertainty handling, particularly in dynamic environments where both spatial and temporal factors are continuously evolving. In our evaluation, we selected $\{l_{space}, l_{time}, \sigma_0\} = \{5, 3600, 5\}$ as parameter values, as this set was validated through multiple trials to better match the variations observed in the dynamic environment during the experiment.

C. Results

1) Monitoring path and estimated temperature: To evaluate the performance of our proposed method in dynamic environments, we selected a period during which significant temperature changes occurred. Based on the temperature variation data collected by the 8 fixed sensors from 8:00 AM to 12:00 PM on June 12, 2024, we observed a noticeable temperature rise at all 8 locations before 10:10 AM due to prolonged sunlight exposure. Subsequently, the temperature decreased following the activation of the air conditioning system, as shown in Fig. 4. Therefore, we used the dataset obtained from 10:00 AM to 10:40 AM to simulate the dynamic temperature changes.

Fig. 5 shows the robot movement path and model data at three specific time points: 10:16:00, 10:20:40, and 10:37:20. In Fig. 5, the top row of each set represents the temperature distribution predicted by the model at the respective time, while the bottom row shows the model's uncertainty distribution. In our experiment, the ST-GPR model predicted temperature changes for the next 40 seconds. Given that the robot's scanning frequency(ΔT) was set to once every 20 seconds, the predicted future path consists of 2 segments. The black path in the figure illustrates the robot's most recent 20 movements, while the light-colored segments depict the predicted optimal path at the moment the robot reaches the end of the black path, based on the PUM algorithm. The red segments indicate the robot's current movement and the yellow segments represent the robot's predicted next movement.

PUM selects the path to minimize the predicted uncertainty of all locations, which means it can direct the robot to reduce uncertainty in regions that haven't been observed for a while. However, this does not involve simply moving in one direction until reaching a boundary and then reversing. As seen at 10:20:40 in Fig. 5, the robot first moves to the unobserved lower-left corner before continuing, demonstrating that the system can prioritize unexplored areas even when it does not follow a straightforward path reversal.

To better illustrate the temperature variations, we uniformly selected four points within the experimental area; A(-30,21), B(-15,21), C(0,21), and D(15,21) shown in Fig. 2. We then compared the actual temperature changes at these points with the predicted temperature changes over time. Fig. 6 shows the results. In Fig. 6, we highlight the confidence interval $\hat{y}(\mathbf{x}^*) \pm \frac{1}{4}\sigma$ using gray shading. As shown in this figure, the actual temperatures at all four points fell within the confi-

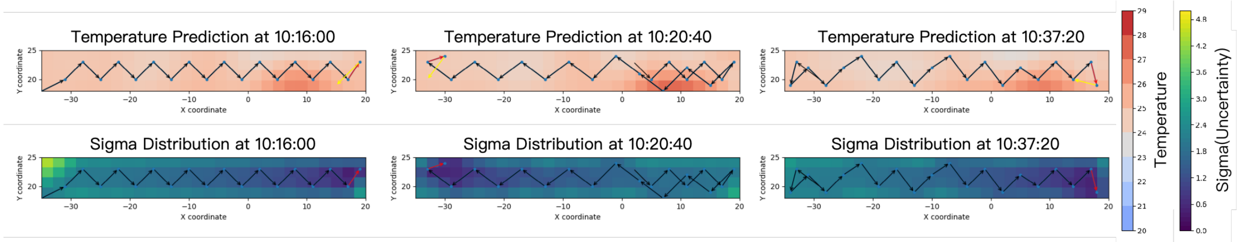

Fig. 5: Robot movement path, predicted temperature and uncertainty distribution

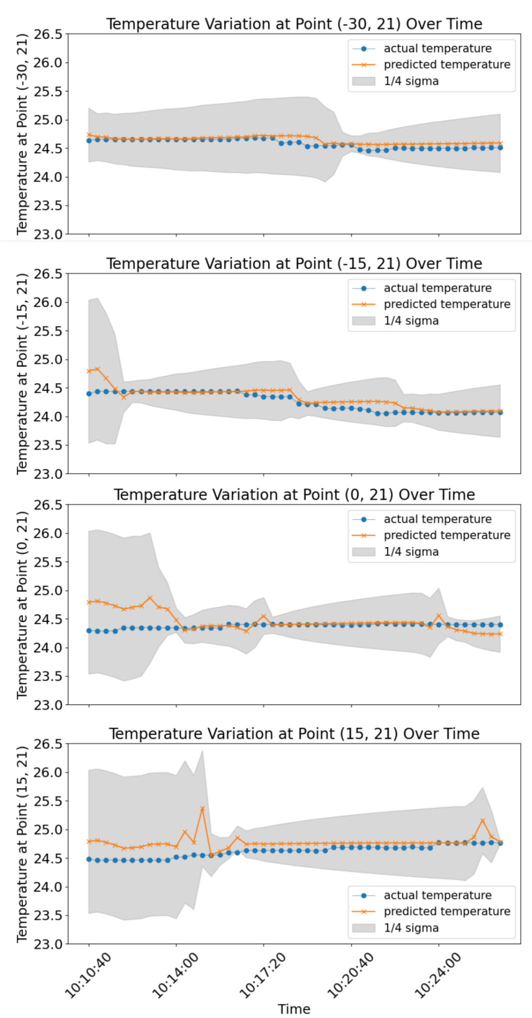

Fig. 6: Time variation of predicted temperatures

dence interval during the period from 10:10:00 to 10:40:00. Additionally, when the robot moved near the points, the width of the confidence interval was visibly shrank, indicating a reduction in uncertainty. For instance, the robot measured the temperature at point A(-30,24) at 10:20:40 in Fig. 5, which caused the uncertainty at point A to drop to its lowest level at that moment. Conversely, during periods when the robot did not visit point A or nearby locations, the width of the confidence interval at A gradually increased over time,

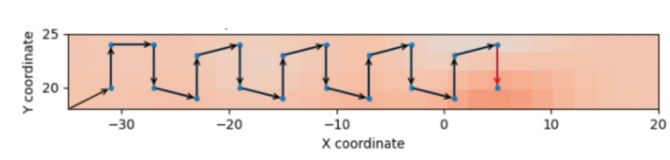

(a) Fixed Path at 10:16:00

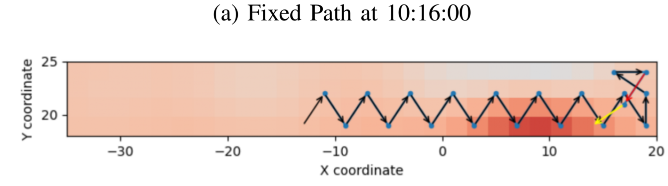

(b) NHU Path at 10:22:00 When Local Optimal Occurred

Fig. 7: Example of monitoring paths by fixed path and next-highest-uncertain path

reflecting the growing uncertainty.

2) Comparison among path planing methods: In this subsection, we compare the results of PUM with the following path planning methods.

Fixed path: In this method, the robot moves on a fixed path X_F to ensure that the robot's scanning range covers the entire experimental area. In this evaluation, we set the fixed path as shown in Fig. 7(a). In this path, the robot moves from left to right at a speed of 0.1 grid units per second. When the robot approaches the right boundary, it reverses direction and moves to the left. This fixed path approach ensures that the robot systematically covers all areas in the environment, reducing the likelihood of leaving any areas unsampled for extended periods. By comparing PUM with this method, we demonstrate the effectiveness of considering uncertainty.

Next-Highest-Uncertain path(NHU): In this method, the robot moves to the point with the highest σ value within its reachable range. That is, this method selects the paths $\mathcal{C}_{NHU}$ according to the following equation.

$$\mathcal{C}_{NHU} = \{z_i \mid z_i = \arg\max_{z \in Z_i} \sigma(z),\, i \in [t, t+H]\} \tag{9}$$

where Z_i indicates the set of locations the robot can reach at time i. In this method, the robot can effectively reduce their corresponding σ values by monitoring at these high-uncertainty locations. By comparing PUM with this method, we demonstrate the effectiveness of considering not only the current uncertainty but also future uncertainty.

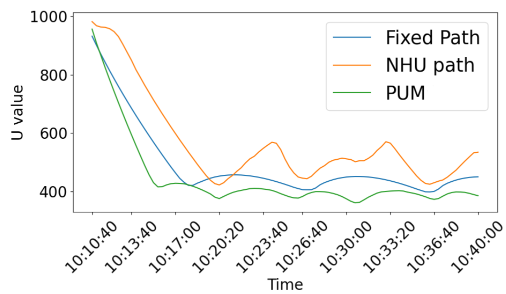

Fig. 8: Time variation of total uncertainty (U)

For evaluation, we compare the U values calculated by Eq. (6) and the results are shown in Fig. 8. The figure demonstrates a consistent trend across all three methods, with an initial rapid decline in U value, particularly between 10:10:40 and 10:17:00. This sharp drop indicates an effective reduction in model uncertainty during the early stages of exploration, as the robot collects new data and refines its understanding of the environment. Notably, around 10:17:00, the U value begins to fluctuate, indicating an inability to maintain low uncertainty over time. These fluctuations arise from the inherent variability in how effectively the robot reduces uncertainty based on its sampling strategy and the spatial-temporal characteristics of the environment.

For the fixed path method, the oscillations are mild, indicating steady but gradual reductions in uncertainty. The robot systematically covers the entire area, but without targeting regions of high uncertainty, resulting in slower reductions in the U value. In contrast, the NHU method shows more pronounced oscillations, as it targets the highest uncertainty points at each step. While this approach leads to reductions when these points are sampled, it can cause fluctuations as the robot frequently shifts between points, leading to local optima and extended periods of higher uncertainty. For instance, Fig.7(b) shows the robot briefly hovering around the right-side region around 10:22:00, which is also evidenced by the significant increase in U value in Fig. 8.

The PUM method, however, outperforms both Fixed Path and NHU by achieving a rapid initial reduction in uncertainty. It achieved the minimum total uncertainty in 360 seconds, compared to 520 seconds for the Fixed Path and 620 seconds for NHU, translating to time savings of 30.77% and 41.94%, respectively. In the later stages of the experiment, PUM further reduced total model uncertainty by 7.91% and 9.25% compared to Fixed Path and NHU, respectively. The minor fluctuations in U value observed in PUM reflect the dynamic nature of the environment but are effectively managed by predicting future high-uncertainty regions, allowing the method to maintain a lower overall uncertainty.

As a result, PUM achieves both fast and sustained reductions in uncertainty, making it the most efficient of the three methods in terms of minimizing model uncertainty.

IV. Conclusion

In this paper, we proposed and evaluated a PUM method for path planning in dynamic environments, aimed at minimizing uncertainty in GPR models for environmental monitoring. The PUM method demonstrated superior performance by effectively balancing exploration and exploitation, enabling the robot to predict and prioritize high-uncertainty regions for future sampling. The experiments demonstrated that PUM not only ensures that the actual temperatures fall within the model's confidence intervals, but also more effectively reduces the prediction model's uncertainty, thereby enhancing the efficiency of environmental monitoring.

For future work, we plan to address the limitations observed when using a uniform set of kernel parameters across the entire environment. Our experiments showed that local factors such as windows and air conditioning units can lead to asynchronous temperature changes across different regions, resulting in prediction errors when a single set of parameters is applied. To improve the model's accuracy, we aim to dynamically adjust the kernel parameters to account for these local variations, thereby further reducing the GPR model prediction errors.

References

[1] M. Pan, C. Chen, X. Yin, and Z. Huang, "UAV-aided emergency environmental monitoring in infrastructure-less areas: Lora mesh networking approach," *IEEE Internet of Things Journal*, vol. 9, no. 4, pp. 2918–2932, 2021.

[2] Y.-C. Lin and W.-F. Cheung, "Developing wsn/bim-based environmental monitoring management system for parking garages in smart cities," *Journal of Management in Engineering*, vol. 36, no. 3, p. 04020012, 2020.

[3] S. L. Ullo and G. R. Sinha, "Advances in smart environment monitoring systems using iot and sensors," *Sensors*, vol. 20, no. 11, p. 3113, 2020.

[4] T. Sood, P. Janssen, and C. Miller, "Spacematch: Using environmental preferences to match occupants to suitable activity-based workspaces," *Frontiers in Built Environment*, vol. 6, p. 113, 2020.

[5] M. Dunbabin and L. Marques, "Robots for environmental monitoring: Significant advancements and applications," *IEEE Robotics & Automation Magazine*, vol. 19, no. 1, pp. 24–39, 2012.

[6] L. Schmid, M. Pantic, R. Khanna, L. Ott, R. Siegwart, and J. Nieto, "An efficient sampling-based method for online informative path planning in unknown environments," *IEEE Robotics and Automation Letters*, vol. 5, no. 2, pp. 1500–1507, 2020.

[7] G. Hitz, E. Galceran, M.-È. Garneau, F. Pomerleau, and R. Siegwart, "Adaptive continuous-space informative path planning for online environmental monitoring," *Journal of Field Robotics*, vol. 34, no. 8, pp. 1427–1449, 2017.

[8] J. P. Fentanes, I. Gould, T. Duckett, S. Pearson, and G. Cielniak, "3D soil compaction mapping through kriging-based exploration with a mobile robot," *IEEE Robotics and Automation Letters*, vol. 3, no. 4, pp. 3066–3072, 2018.

[9] H. Zhu, J. J. Chung, N. R. Lawrance, R. Siegwart, and J. Alonso-Mora, "Online informative path planning for active information gathering of a 3d surface," in *2021 IEEE International Conference on Robotics and Automation (ICRA)*. IEEE, 2021, pp. 1488–1494.

[10] M. Schwenzer, M. Ay, T. Bergs, and D. Abel, "Review on model predictive control: An engineering perspective," *The International Journal of Advanced Manufacturing Technology*, vol. 117, no. 5, pp. 1327–1349, 2021.

[11] Y. Geng, M. Yuan, H. Tang, Y. Wang, Z. Wei, B. Lin, and W. Zhuang, "Robot-based mobile sensing system for high-resolution indoor temperature monitoring," *Automation in Construction*, vol. 142, p. 104477, 2022.